RSC Applied Polymers

PAPER

View Article Online
View Journal

Cite this: DOI: 10.1039/d6lp00094k

Hydrophobically modified poly(acrylic acid) coatings on silicone hydrogel contact lenses

Jimin Yoo,[a] Minjoong Shin, †[a] Si Chul Rho,[b] Minho Jung*[b] and Myungeun Seo *[a,c]

Received 18th March 2026,
Accepted 21st May 2026

DOI: 10.1039/d6lp00094k

rsc.li/rscapplpolym

Silicone hydrogel (Si-Hy) contact lenses offer high oxygen permeability and mechanical durability but often exhibit poor surface wettability due to the intrinsic hydrophobicity of silicone components. We investigated hydrophobically modified poly(acrylic acid) (PAA)-based amphiphilic copolymers as coating materials for Si-Hy lenses to effectively cover their chemically heterogeneous surface. A series of statistical copolymers were synthesized by copolymerizing acrylic acid with alkyl acrylates bearing linear alkyl side chains with a varying number of carbon atoms from 6 to 12. By varying molecular weight, hydrophobic content, and alkyl chain length, we examined how hydrophobic interactions influence solution behavior, interfacial properties, and coating performance. Increasing hydrophobic content enhanced anchoring to silicone domains, whereas excessive hydrophobicity promoted intermolecular association of alkyl chains. Among the copolymers studied, the poly(acrylic acid-*co*-octyl acrylate) copolymer exhibited the lowest contact angle and friction coefficient, indicating improved wettability and lubrication. These results demonstrate that amphiphilic coatings with optimized hydrophobic contents and alkyl chain lengths can effectively improve the interfacial properties of Si-Hy lenses.

Introduction

Silicone-based hydrogel (Si-Hy) contact lenses offer high oxygen permeability and enhanced mechanical durability compared to hydrophilic-only soft hydrogel lenses.[1–3] Incorporation of silicone materials, such as polydimethylsiloxane (PDMS), allows more oxygen to pass through the lens and can help reduce the risk of corneal hypoxia during lens wear.[4–8] In commercial Si-Hy lenses, silicone polymers are typically combined with hydrophilic polymers, such as poly(2-hydroxyethyl methacrylate) and poly(*N*-vinyl pyrrolidone), within an interpenetrating polymer network (IPN).[9–11] The intertwined co-network maintains dimensional stability and optical transparency by preventing phase separation between the drastically different silicone and hydrophilic polymers. However, the inherently hydrophobic nature of silicone chains reduces surface wettability and repels moisture from the lens surface, compromising wearer comfort, particularly for those with dry-eye symptoms.[12,13]

A coating on a contact lens primarily functions as an interface-modifying layer that tailors interactions with the surrounding tear film. To be effective, such a coating must simultaneously provide strong affinity to the lens surface, excellent lubricity, long-term comfort, and non-irritating biocompatibility—all without altering the bulk optical or mechanical properties of the lens.[14] Surface-active molecules have been incorporated during polymerization or applied post-polymerization as coating additives to enhance lubricity and wettability.[15,16] Hydrophilic polymers such as poly(ethylene glycol), poly(acrylic acid), and poly(2-methacryloyloxyethyl phosphorylcholine) have been employed for this purpose.[14,17,18] However, coatings composed of a single hydrophilic component often exhibit limited compatibility with the chemically heterogeneous Si-Hy lens surface, which contains both hydrophilic and hydrophobic domains originating from hydrogel and silicone segments.

Recent developments in amphiphilic random copolymers highlight their unique ability to interact adaptively with complex interfaces and motivate their application in Si-Hy lens coatings. While each copolymer chain can have a drastically different sequence of hydrophobic and hydrophilic repeating units, such heteropolymers have been shown to recognize and interact with chemically heterogeneous environments, preserving protein function and enabling selective transport through lipid bilayers.[19,20] Despite the broad sequence distribution, amphiphilic random copolymers have been reported to form

[a]*Department of Chemistry, Korea Advanced Institute of Science and Technology (KAIST), Daejeon 34141, Republic of Korea. E-mail: seomyungeun@kaist.ac.kr*
[b]*Interojo Inc., Pyeongtaek 17791, Republic of Korea. E-mail: mhjung@interojo.com*
[c]*KAIST Institute for the Nanocentury, Korea Advanced Institute of Science and Technology (KAIST), Daejeon 34141, Republic of Korea*
†Current address: Department of Chemical and Biological Engineering, Northwestern University, Evanston, Illinois 60208, USA.

micelles in aqueous media and lyotropic mesophases at higher concentrations *via* association between hydrophobic pendants, such as alkyl side chains.[21–24] While the average copolymer composition primarily determines the interfacial curvature of the assemblies, similar to a diblock copolymer analog, the length scale of the assemblies follows that of the side chains, leading to much broader interface coverage per polymer.[25,26] In addition, the higher modulus of the lyotropic mesophase with the increasing degree of polymerization suggests that the association between copolymers becomes stronger collectively by involving more side chains. Together, these studies indicate that amphiphilic copolymers bearing hydrophobic pendants can stabilize adsorption onto hydrophobic surface domains while maintaining overall aqueous compatibility—an interfacial requirement that aligns precisely with the heterogeneous architecture of Si-Hy lenses.

In this work, we investigated hydrophobically modified poly(acrylic acid)s containing statistically distributed acrylic acid and alkyl acrylate repeating units as coating materials for Si-Hy lenses (Fig. 1a). Hydrophobically modified poly(acrylic acid)s are commercially available materials used as viscosity modifiers to thicken aqueous solutions, emulsifiers, and drug carriers.[27–31] We synthesized a series of amphiphilic statistical copolymers by copolymerizing acrylic acid (AA) with an alkyl acrylate (*x*A) monomer to produce P(AA-*co*-*x*A), in which the number of carbon atoms in the alkyl side chain (C_n) varied from 6 (hexyl) to 12 (dodecyl). We found that the viscosity and surface tension of their aqueous solutions, as well as the contact angles of the coated surfaces, were significantly affected by the copolymer's molar composition and alkyl chain length. While surface energy generally decreased with increasing alkyl chain weight fraction, excessive alkyl chain loading led to a rough surface, presumably due to alkyl domain formation. When applied to commercial Si-Hy lenses, both the contact angle and friction coefficient were minimized at an intermediate alkyl chain length, suggesting that the heterogeneous lens surface can be effectively covered with an appropriately balanced hydrophobic content (Fig. 1b). We envision that the amphiphilic copolymer can serve as a versatile platform for multifunctional lens coating materials through further side-chain engineering, incorporating various functionalities.

Results and discussion

Copolymer synthesis

Hydrophobically modified PAAs were synthesized *via* radical copolymerization of AA with alkyl acrylates (Scheme 1). To systematically investigate the influence of molecular weight and hydrophobic composition, reversible addition–fragmentation chain-transfer (RAFT) copolymerization of AA and dodecyl acrylate (DDA) was conducted using 2-(dodecylthiocarbonothioylthio)-2-methylpropionic acid (DDMAT) as the chain transfer agent (CTA). This approach enabled precise control of the degree of polymerization (N = 200–1600) and the hydrophobic content (0–10%) (see Table 1 for the characterization details). RAFT copolymerization kinetics were monitored for a representative feed ratio of [AA] : [DDA] = 90 : 10 (Fig. S1). Although the monomers exhibited different consumption

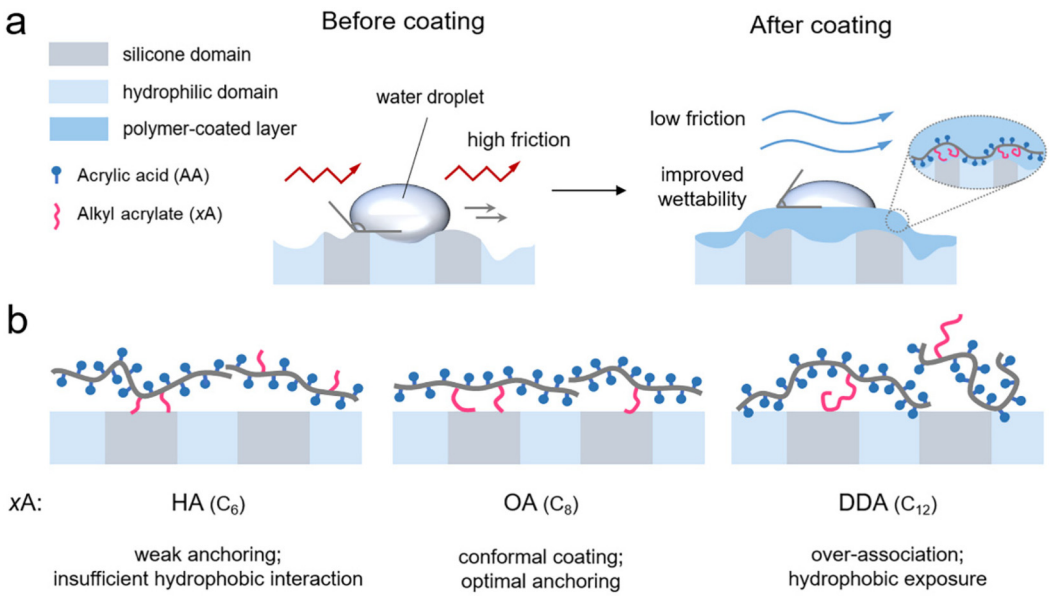

Fig. 1 (a) Schematic illustration of the amphiphilic copolymer coating on a chemically heterogeneous silicone hydrogel (Si-Hy) lens surface. The surface consists of silicone-rich and hydrophilic domains. A water droplet is placed on the surface to illustrate differences in wettability before and after coating. The darker blue region represents a hydrated polymer layer formed after coating. (b) Effect of alkyl side-chain length on interfacial anchoring and coating behavior: hexyl acrylate (HA) exhibits weak anchoring with partially exposed chains, octyl acrylate (OA) achieves balanced and uniform anchoring, and dodecyl acrylate (DDA) shows limited anchoring with increased chain exposure due to increased hydrophobic association.

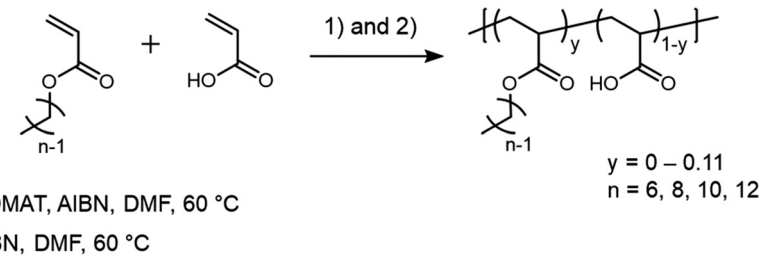

Scheme 1 Synthetic routes for P(AA-*co*-*x*A) prepared *via* RAFT (1) and free-radical copolymerization (2).

Table 1 Synthesis and characterization of P(AA-*co*-DDA)s produced *via* RAFT copolymerization

Sample name	Feed composition [AA] : [DDA] : [CTA]	Conv.$_{AA}$ [a] (%)	Conv.$_{DDA}$ [a] (%)	$M_{n,theo}$ [a] (kg mol^{-1})	$i_{DDA,theo}$ [b] (mol%)	$i_{DDA,NMR}$ [c] (mol%)
PAA_{190}	[200] : [0] : [1]	95	—	14	0	0
P(AA_{184}-*co*-DDA_9)	[190] : [10] : [1]	97	85	15	4	6
P(AA_{176}-*co*-DDA_{17})	[180] : [20] : [1]	98	87	17	9	9
PAA_{344}	[400] : [0] : [1]	86	—	25	0	0
P(AA_{353}-*co*-DDA_{20})	[380] : [20] : [1]	93	100	30	5	5
P(AA_{346}-*co*-DDA_{40})	[360] : [40] : [1]	96	100	34	11	9
PAA_{528}	[600] : [0] : [1]	88	—	38	0	0
P(AA_{536}-*co*-DDA_{30})	[570] : [30] : [1]	94	100	48	5	5
P(AA_{529}-*co*-DDA_{60})	[540] : [60] : [1]	98	100	52	11	11
PAA_{800}	[800] : [0] : [1]	100	—	58	0	0
P(AA_{730}-*co*-DDA_{40})	[760] : [40] : [1]	96	100	62	6	5
P(AA_{648}-*co*-DDA_{80})	[720] : [80] : [1]	90	100	66	10	9

[a] Determined by ^{1}H NMR spectroscopy. [b] Determined by ^{1}H NMR spectroscopy based on conversion. [c] Determined by ^{1}H NMR spectroscopy based on the composition of each monomer in polymers.

rates, both showed linear pseudo-first-order kinetics, consistent with a well-controlled RAFT process. To explore the effect of alkyl side-chain length, additional hydrophobically modified PAAs were synthesized *via* free radical copolymerization of AA with hexyl acrylate (HA), octyl acrylate (OA), and decyl acrylate (DA), while avoiding sulfur-containing CTAs due to concerns regarding residual color and odor in lens applications (Table 2). DA was synthesized following the procedure in the literature[32] (Fig. S2). Because the hydrophobic contribution varies with alkyl length, the feed compositions were selected to maintain a constant hydrophilic–lipophilic balance (HLB) calculated according to Griffin's method[33] to ensure a constant value. All copolymerizations proceeded with monomer conversions above 80%. Composition analysis using ^{1}H NMR showed that the copolymer composition was similar to the initial feed ratio, indicating that the hydrophobic content can be controlled by the feed composition (Fig. S3). We attempted to analyze the synthesized copolymers using size exclusion chromatography but observed poor filterability and unstable elution behavior, presumably because of their partial solubility in eluents and polymer-column interactions. Detailed information, including feed composition and characterization of the polymers, is provided in Table 2.

Hydrophobic content and molecular weight effect

To identify an optimal polymer design for lens coatings, we investigated how the hydrophobic content and molecular weight of P(AA-*co*-DDA) influence the solution behavior and surface characteristics. As shown in Fig. 2a and b, the viscosity of P(AA-*co*-DDA) aqueous solutions tends to increase with both the theoretical molecular weight ($M_{n,theo}$) and the hydrophobic content (i_{DDA}). At both 0.01 and 0.05 wt%, the viscosity exhibi-

Table 2 Synthesis and characterization of P(AA-*co*-*x*A)s produced *via* free radical copolymerization

Sample name	Feed composition [AA] : [*x*A] : [AIBN]	Conv.$_{AA}$ [a] (%)	Conv.$_{xA}$ [a] (%)	$i_{xA,theo}$ [b] (mol%)	$i_{xA,NMR}$ [c] (mol%)
P(AA_{1166}-*co*-HA_{48})	[2880] : [120] : [1]	81	80	4	4
P(AA_{1324}-*co*-OA_{42})	[2910] : [90] : [1]	91	93	3	4
P(AA_{1316}-*co*-DA_{35})	[2925] : [75] : [1]	90	93	2	2
P(AA_{1220}-*co*-DDA_{30})	[2940] : [60] : [1]	83	100	2	2

[a] Determined by ^{1}H NMR spectroscopy. [b] Determined by ^{1}H NMR spectroscopy based on conversion. [c] Determined by ^{1}H NMR spectroscopy based on the composition of each monomer in the polymers.

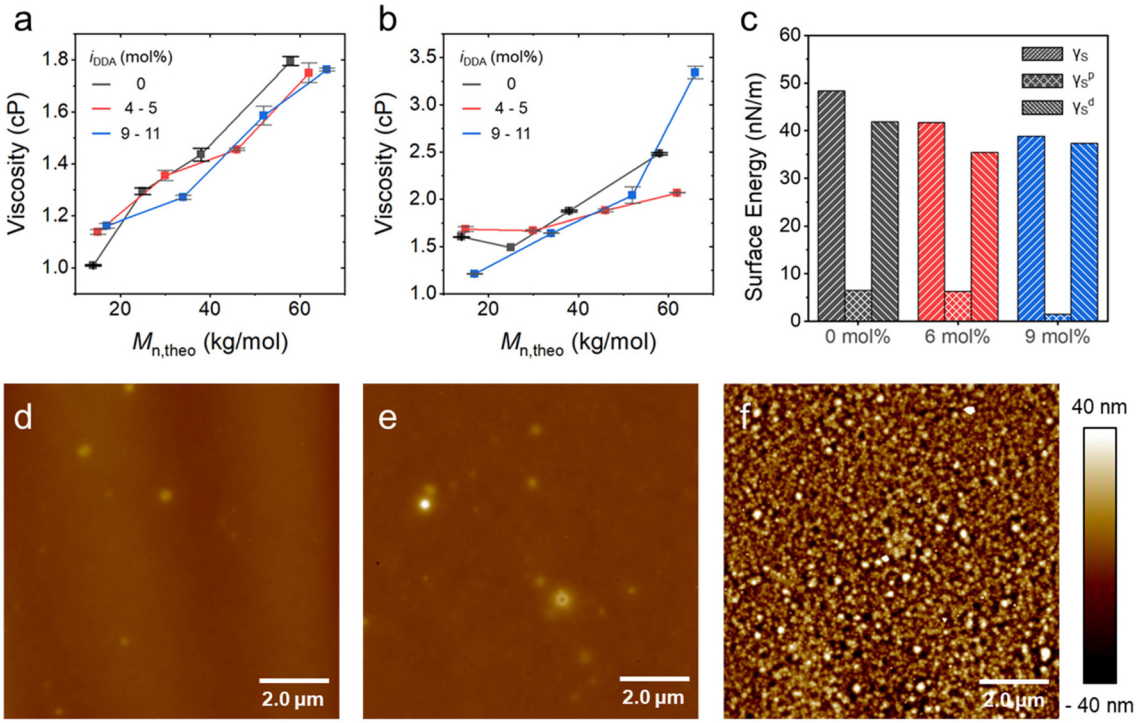

Fig. 2 (a) Viscosity of P(AA-*co*-DDA) aqueous solutions at 0.01 wt% and (b) 0.05 wt%. (c) Total surface energy (γ_s) of the coated Si wafers and its polar (γ_s^p) and dispersive (γ_s^d) components calculated using the Owens–Wendt method based on the contact angle data. (d–f) AFM image of a Si wafer coated with (d) PAA_{344} (i_{DDA} = 0%), (e) $P(AA_{353}$-*co*-$DDA_{20})$ (i_{DDA} = 6%), and (f) $P(AA_{346}$-*co*-$DDA_{40})$ (i_{DDA} = 9%).

ted a clear dependence on molecular weight, consistent with the molecular-weight scaling behavior described by the Mark–Houwink relationship.[34,35] A sharp increase in viscosity was observed for the copolymer with i_{DDA} = 9% and 66 kg mol^{-1} at a 0.05 wt% concentration, indicating that substantial intermolecular association involving the alkyl side chains led to associative thickening.

We measured the contact angles of drop-cast copolymer films on silicon wafer substrates as a function of i_{DDA} using diiodomethane (DIM) and glycerol as hydrophobic and hydrophilic probe liquids, respectively (Fig. S4). Higher-molecular-weight copolymers generally exhibited lower contact angles than the lower-molecular-weight set, suggesting improved film uniformity and enhanced substrate wetting. Significantly lower root mean-square (RMS) values for higher-molecular-weight copolymer coatings except for $P(AA_{346}$-*co*-$DDA_{40})$ with the highest i_{DDA} = 9 mol%, determined by atomic force microscopy (AFM) imaging, supported higher film quality (Fig. S5 and Table S1). The DIM contact angles were higher than those measured with glycerol, reflecting differences in probe–liquid polarity and solid–liquid interactions. Fig. 2c shows the calculated surface energy (γ_s) of the higher-molecular-weight-copolymer-coated wafers based on the Owens–Wendt model,[36,37] which decreases with increasing i_{DDA} over the investigated composition range. A decrease in both the polar (γ_s^p) and dispersive (γ_s^d) components is consistent with reduced surface polarity due to an increased population of dodecyl chains on the surface at the cost of acid number reduction. AFM imaging of surfaces coated with higher-molecular-weight samples showed uniform surface coverage by the PAA homopolymer (i_{DDA} = 0%, Fig. 2d) and the copolymer with moderate hydrophobic content (i_{DDA} = 6%, Fig. 2e), with relatively smooth, continuous textures and a RMS roughness of 1.5 nm. A further increase in hydrophobic content to i_{DDA} = 9% resulted in a distinct morphology characterized by heterogeneous granular textures (Fig. 2f). We posit that the formation of hydrophobic domains *via* alkyl–alkyl association occurs above a critical hydrophobic content. We also note that the opposing trend compared to the intermediate i_{DDA} regime (*i.e.*, increasing γ_s^p and decreasing γ_s^d) would also be related to the segregation of hydrophobic domains from the uniformly mixed state. As lens coating requires the contact angle not to increase, we decided to further investigate copolymers with low hydrophobic content.

Effect of alkyl length

We then investigated the effect of hydrophobic side-chain length at the air–water interface by evaluating the surface tension of copolymer aqueous solutions. We synthesized a series of P(AA-*co*-*x*A) copolymers with C_n ranging from 6 to 12 by free radical copolymerization, while maintaining a constant hydrophilic–lipophilic balance (HLB) of 11–12, which corresponds to i_{xA} = 4 (HA) − 2 (DDA) mol%. At a 0.05 wt% concentration, the surface tension of the copolymer solutions decreased markedly with increasing alkyl length, reflecting

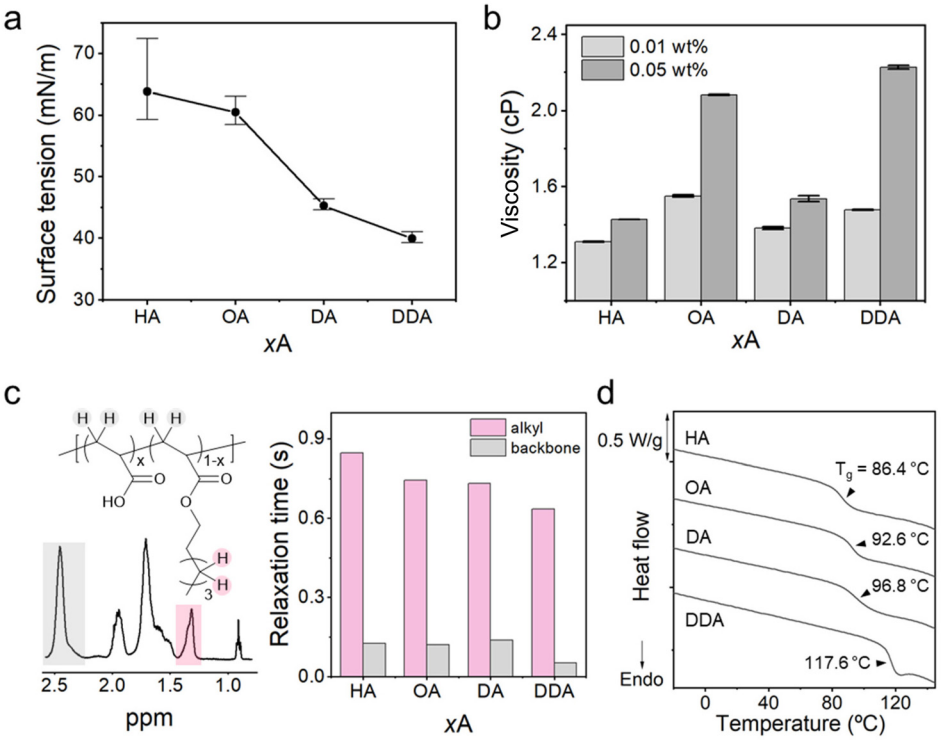

Fig. 3 (a) Surface tension of 0.05 wt% P(AA-*co*-*x*A) aqueous solutions at the air–water interface. (b) Viscosity of 0.01 and 0.05 wt% P(AA-*co*-*x*A) aqueous solutions. (c) T_1 and T_2 relaxation times measured using ^{1}H NMR in CD_3OD (25 °C). (d) DSC thermograms of P(AA-*co*-*x*A) in the second heating cycle (10 °C min^{-1}, N_2).

stronger adsorption of longer side chains at the air–water interface (Fig. 3a). Increasing alkyl length also enhanced cohesive interactions among hydrophobic segments, as evidenced by thickening of the copolymer solutions (Fig. 3b). A non-monotonic dependence on alkyl chain length was observed in solution viscosity at both 0.01 and 0.05 wt%, with a decline at C_n = 10 (DA). While we are not certain about the origin of this phenomenon, we posit that the copolymer may undergo a conformational change from a relatively open state to a micelle-like form with segregated alkyl chains within it above a critical hydrophobic content. While relatively fewer alkyl chains may contribute to intermicellar interactions, further increasing alkyl length would increase solution viscosity again, particularly at higher concentrations, due to greater overlap.

The ^{1}H NMR transverse relaxation times (T_2) measured in CD_3OD decreased from 0.85 s (HA) to 0.63 s (DDA), confirming slower segmental dynamics of the longer alkyl side-chains because of alkyl chain segregation and intermolecular association (Fig. 3c and Table S2). In contrast, the backbone T_2 values showed no clear variation with alkyl length except for the notable decrease in the DDA case, suggesting that the restricted mobility primarily originates from the alkyl side chains rather than the main chain. In addition, conventional ^{1}H NMR spectra acquired in D_2O showed a more pronounced reduction in alkyl peak integration compared to CD_3OD when DA was used (Fig. S6), suggesting the onset of alkyl chain association in aqueous environments consistent with the viscosity data. A gradual increase in the glass transition temperature (T_g) of the copolymers was observed by differential scanning calorimetry (DSC), ranging from 86 °C for HA to 118 °C for DDA (Fig. 3d). This is also consistent with restricted chain mobility due to stronger alkyl chain association in the bulk state. Note that significantly increased T_g in P(AA-*co*-DDA), combined with T_2 reduction, suggests that strong alkyl–alkyl association can hinder backbone dynamics in bulk and also in solution. AFM images of silicon wafers coated with the P(AA-*co*-*x*A) showed continuous and uniform polymer layers with substantially lower surface roughness compared to the P(AA-*co*-DDA) series with high DDA loading, presumably because the formation of large hydrophobic domains was suppressed under lower hydrophobicity (Fig. S7). The RMS roughness showed no systematic dependence on alkyl chain length across the HA–DDA series, indicating that the coating morphology is largely preserved at comparable hydrophobic contents. These results suggest that differences in wettability and friction primarily originate from surface chemistry and interfacial interactions rather than coating topography.

Si-Hy lens coating

The analyses of P(AA-*co*-*x*A)s in aqueous solution and at the interface showed that the extent of surface hydrophobicity and alkyl chain association can be adjusted by the *x*A mol fraction in the copolymer and alkyl length. We applied the P(AA-*co*-*x*A)s produced by free radical polymerization as coating materials

for commercial Si-Hy contact lenses. The Si-Hy contact lenses were subjected to solvent pretreatment, followed by polymer coating, surfactant post-treatment, and final rinsing with deionized water. Detailed experimental conditions are provided in the SI (Fig. S8). We determined the water contact angle and friction coefficient of the coated lens surface to evaluate their performance and summarized the results in Fig. 4a and b and Table S3. Previous studies reported friction coefficients of silicone hydrogel contact lenses of ~0.25–0.30 under aqueous lubrication conditions[38] and ~0.05–0.09 in blink-model experiments using artificial tear solutions.[39] The present coatings exhibit lower friction values of 0.028–0.03, indicating excellent lubrication performance.

Among the copolymers tested, P(AA-*co*-OA) showed the most pronounced improvement, exhibiting both the lowest contact angle and the lowest friction coefficient. It is striking that P(AA-*co*-OA) outperforms the others in both properties and particularly lowers the contact angle by 28–44°. Given that P(AA-*co*-HA) exhibited higher surface tension than P(AA-*co*-OA) and noticeably lower viscosity at 0.05 wt%, the result suggests that the short hexyl side-chain in HA cannot provide sufficient hydrophobic interaction with the silicone domain on the lens surface to be anchored stably. Increasing the alkyl length beyond OA also seems detrimental, as a longer alkyl chain may favor the air–polymer interface over the polymer-lens, resulting in a higher contact angle. We also note that the intermediate mobility of the OA side chain may provide more fluidic surface environments than those of the longer alkyl analogues, allowing the side chain to move and flip, thereby enhancing lubrication properties. The P(AA-*co*-OA)-coated lens maintained optical clarity without visible defects and could not be distinguished from the uncoated lens (Fig. 4b and c), demonstrating that the thin polymer coating does not compromise transparency.

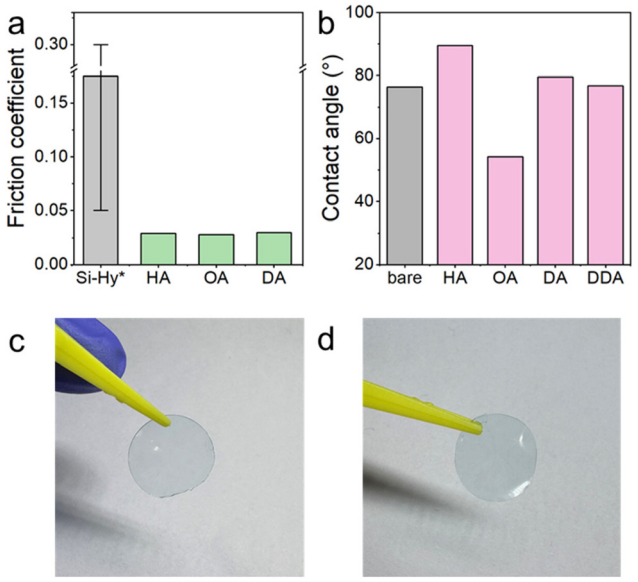

Fig. 4 (a) Friction coefficient and (b) water contact angles of P(AA-*co*-*x*A)-coated Si-Hy lens. (c) Image of an uncoated Si-Hy lens and (d) a P(AA-*co*-OA)-coated Si-Hy lens. Friction coefficients of the uncoated Si-Hy lens (*) reported in the literature[38,39] for silicone hydrogel lenses under aqueous or tear-like lubrication conditions were used.

Conclusion

We explored hydrophobically modified PAAs as coating materials on Si-Hy contact lenses. Hydrophobic alkyl side chains were incorporated into PAA by copolymerizing AA with *x*A bearing different alkyl groups as a hydrophobic comonomer to match the hydrophobic surface characteristics of the silicone polymer, thereby improving surface performance and wearer comfort. By systematically varying the copolymer molecular weight, *x*A fraction, and alkyl side-chain length, we found that, while the hydrophobic interaction became stronger with increasing *x*A mol fraction and alkyl length, segregation of the alkyl chains, followed by intermolecular association and strong adsorption at the air–water interface, was observed above a threshold. On a Si-Hy lens surface, P(AA-*co*-OA) bearing the intermediate alkyl side chain outperformed the other copolymers at the same HLB but with different alkyl lengths. Our findings suggest that a hydrophilic-rich amphiphilic copolymer that can provide a highly fluidic surface and adequately interact with the silicone polymer surface without noticeable domain formation can preserve optical transparency while enhancing surface wettability and lubrication, making them promising candidates for next-generation contact lens coatings.

Author contributions

Jimin Yoo: conceptualization, investigation, visualization, writing – original draft, and writing – review & editing. Minjoong Shin: investigation and methodology. Si Chul Rho: funding acquisition and supervision. Minho Jung: conceptualization, supervision, and writing – review & editing. Myungeun Seo: conceptualization, supervision, funding acquisition, and writing – review & editing.

Conflicts of interest

The authors declare no competing financial interest.

Data availability

The data supporting this article have been included as part of the supplementary information (SI). Supplementary information: materials and methods including experimental details, Tables S1–S3 including RMS roughness of the coated surfaces, relaxation times, and lens coating performances, Fig. S1–S8 including NMR spectra of decyl acrylate and P(AA-*co*-*x*A) copolymers, contact angle data, AFM images, and the lens coating procedure. See DOI: https://doi.org/10.1039/d6lp00094k.

Acknowledgements

This work was supported by INTEROJO INC. and by the National Research Foundation of Korea (NRF) grant funded by the Korean government (MSIT) (RS-2023-NR077111).

References

1 F. Stapleton, S. Stretton, E. Papas, C. Skotnitsky and D. F. Sweeney, *Ocul. Surf.*, 2006, **4**, 24–43.
2 C. S. A. Musgrave and F. Fang, *Materials*, 2019, **12**, 261.
3 P. C. Nicolson and J. Vogt, *Biomaterials*, 2001, **22**, 3273–3283.
4 D. F. Sweeney, *Eye Contact Lens*, 2013, **39**, 53–60.
5 N.-P.-D. Tran, C.-C. Ting, C.-H. Lin and M.-C. Yang, *Polymers*, 2020, **12**, 2087.
6 C. Maldonado-Codina, P. B. Morgan, C. M. Schnider and N. Efron, *Optom. Vis. Sci.*, 2004, **81**, 911–921.
7 N. A. Brennan, M. L. Coles and J. H. Ang, *Clin. Exp. Optom.*, 2006, **89**, 18–25.
8 B. M. Aakre, A. E. Ystenaes, M. J. Doughty, O. Austrheim, B. Westerfjell and M. T. A. Lie, *Ophthalmic Physiol. Opt.*, 2004, **24**, 130–141.
9 J. Wang and X. Li, *J. Appl. Polym. Sci.*, 2010, **116**, 2749–2757.
10 R. Ramachandram, E. Albert and R. L. Joseph, *J. Biomed. Opt.*, 2018, **23**, 057005.
11 T. Shimizu, T. Goda, N. Minoura, M. Takai and K. Ishihara, *Biomaterials*, 2010, **31**, 3274–3280.
12 N. Keir and L. Jones, *Eye Contact Lens*, 2013, **39**, 100–108.
13 C. G. Begley, B. Caffery, K. K. Nichols and R. Chalmers, *Optom. Vis. Sci.*, 2000, **77**, 40–46.
14 L. C. Bengani, G. W. Scheiffele and A. Chauhan, *J. Colloid Interface Sci.*, 2015, **445**, 60–68.
15 M. S. Bhamla, W. L. Nash, S. Elliott and G. G. Fuller, *Langmuir*, 2015, **31**, 3820–3828.
16 V. Chandran Suja, A. Verma, E. J. L. Mossige, K. W. Cui, V. Xia, Y. Zhang, D. Sinha, S. Joslin and G. G. Fuller, *J. Colloid Interface Sci.*, 2022, **614**, 24–32.
17 S. K. R. Pillai, S. Reghu, Y. Vikhe, H. Zheng, C. H. Koh and M. B. Chan-Park, *Macromol. Rapid Commun.*, 2020, **41**, 2000175.
18 K. Ishihara, X. Shi, K. Fukazawa, T. Yamaoka, G. Yao and J. Y. Wu, *ACS Appl. Bio Mater.*, 2023, **6**, 3600–3616.
19 B. Panganiban, B. Qiao, T. Jiang, C. DelRe, M. M. Obadia, T. D. Nguyen, *et al.*, *Science*, 2018, **359**, 1239–1243.
20 T. Jiang, A. Hall, M. Eres, Z. Hemmatian, B. Qiao, Y. Zhou, *et al.*, *Nature*, 2020, **577**, 216–220.
21 T. Terashima, T. Sugita, K. Fukae and M. Sawamoto, *Macromolecules*, 2014, **47**, 589–600.
22 Y. Hirai, T. Terashima, M. Takenaka and M. Sawamoto, *Macromolecules*, 2016, **49**, 5084–5091.
23 G. Hattori, M. Takenaka, M. Sawamoto and T. Terashima, *J. Am. Chem. Soc.*, 2018, **140**, 8376–8379.
24 M. Shin, H. Kim, G. Park, J. Park, H. Ahn, D. K. Yoon, *et al.*, *Nat. Commun.*, 2022, **13**, 2433.
25 J. Nam, S. Kwon, Y. G. Yu, H. B. Seo, J. S. Lee, W. B. Lee, *et al.*, *Macromolecules*, 2021, **54**, 8829–8838.
26 S. Kwon, J. Nam, J. W. Chung, M. Seo, W. B. Lee and Y. Kim, *Macromolecules*, 2024, **57**, 7664–7674.
27 O. E. Philippova, D. Hourdet, R. Audebert and A. R. Khokhlov, *Macromolecules*, 1997, **30**, 8278–8285.
28 Ł. Lamch, S. Ronka, I. Moszyńska, P. Warszyński and K. A. Wilk, *Polymers*, 2020, **12**, 1185.
29 S. Riemer, S. Prévost, M. Dzionara, U. Gasser and M. Gradzielski, *Polymer*, 2017, **128**, 78–86.
30 P. Perrin and F. Lafuma, *J. Colloid Interface Sci.*, 1998, **197**, 317–326.
31 S. Chakraborty and P. Somasundaran, *Soft Matter*, 2006, **2**, 850–854.
32 B. Neises and W. Steglich, *Angew. Chem., Int. Ed. Engl.*, 1978, **17**, 522–524.
33 W. C. Griffin, *J. Soc. Cosmet. Chem.*, 1949, **1**, 311–325.
34 P. C. Hiemenz and T. P. Lodge, *Polymer Chemistry*, CRC Press, Boca Raton, 2007.
35 M. Rubinstein and R. H. Colby, *Polymer Physics*, Oxford University Press, Oxford, 2003.
36 D. K. Owens and R. C. Wendt, *J. Appl. Polym. Sci.*, 1969, **13**, 1741–1747.
37 T. Senturk Parreidt, M. Schmid and C. Hauser, *Foods*, 2017, **6**, 31.
38 D. Silva, A. C. Fernandes, T. G. Nunes, R. Colaço and A. P. Serro, *Acta Biomater.*, 2015, **26**, 184–194.
39 C. M. Phan, V. W. Chan, E. Drolle, A. Hui, W. Ngo, S. Bose, *et al.*, *Cont. Lens Anterior Eye*, 2024, **47**, 102129.